Magnetic short-range order and reentrant-spin-glass-like behavior in $CoCr_2O_4$ and $MnCr_2O_4$ by means of neutron scattering and magnetization measurements

K. Tomiyasu,* J. Fukunaga, and H. Suzuki
Department of Applied Physics, School of Science and Engineering, Waseda University, 3-4-1 Ohkubo, Shinjuku, Tokyo 169-8555, Japan

(Received 25 July 2003; revised manuscript received 4 March 2004; published 30 December 2004)

We reinvestigate the ferrimagnetic spiral ordering of the normal spinel ferrimagnets $CoCr_2O_4$ ($T_C \simeq 93$ K) and $MnCr_2O_4$ ($T_C \simeq 51$ K), in which magnetic Co^{2+} and Mn^{2+} ions occupy the *A* sites and magnetic Cr^{3+} ions occupy the *B* sites, by neutron scattering experiments and magnetization measurements on single crystal specimens. Neutron scattering experiments revealed that the fundamental reflections show coherent Bragg peaks at all temperatures below T_C, while the satellite reflections are diffusive even in the lowest temperature phase below T_F ($\simeq 13$ K for $CoCr_2O_4$ and $\simeq 14$ K for $MnCr_2O_4$). These facts indicate the simultaneous formation of a long-range order of the ferrimagnetic component and of a short-range order of the spiral component in the lowest temperature phase. The correlation length of the ferrimagnetic long-range order is estimated to be larger than 50 nm below T_C, while that of the spiral short-range order is estimated to be 3.1 nm at 8 K for $CoCr_2O_4$ and 9.9 nm at 4 K for $MnCr_2O_4$. In magnetization measurements, a reentrant-spin-glass-like behavior of the ferrimagnetic domains was found in the two chromites. In order to explain these magnetic properties comprehensively, we propose the concept of "weak magnetic geometrical frustration;" magnetic geometrical frustration among the *B* sites forming the pyrochlore lattice survives even if magnetic ions occupy the other sublattices (*A* sites). The weak magnetic geometrical frustration leads to the spiral short-range order. Since the magnitude of magnetic moments of Mn^{2+} ions at the *A* sites ($5\mu_B$ spin-only value) is larger than that of Co^{2+} ions at the *A* sites ($3\mu_B$ spin-only value), the degree of magnetic geometrical frustration among the *B* sites in $MnCr_2O_4$ is weaker than that in $CoCr_2O_4$; therefore, the correlation length of the spiral component in $MnCr_2O_4$ (9.9 nm) is larger than that in $CoCr_2O_4$ (3.1 nm). The reentrant-spin-glass-like behavior of the ferrimagnetic domains is caused by freezing and fluctuation of the spiral component.

DOI: 10.1103/PhysRevB.70.214434 PACS number(s): 75.40.−s, 75.60.−d

I. INTRODUCTION

$CoCr_2O_4$ is a cubic normal spinel ferrimagnet ($T_C \simeq 97$ K), in which magnetic Co^{2+} ions occupy the *A* sites and magnetic Cr^{3+} ions occupy the *B* sites.[1] Menyuk *et al.* investigated magnetic ordering below T_C by neutron diffraction experiments and magnetization measurements on a powder specimen and reported the following results.[1] Magnetic order consists of a ferrimagnetic component and a spiral component. The ferrimagnetic component exhibits long-range order at all temperatures below T_C while, as the temperature decreases below T_C, the spiral component exhibits short-range order at $T_t \simeq 86$ K and the spiral short-range order transforms into long-range order at $T_S \simeq 31$ K. Figures 1(a) and 1(b) show the crystal structure and the ferrimagnetic spiral long-range order below T_S, respectively.

However, there are two objections to the Menyuk *et al.* ferrimagnetic spiral long-range order below T_S, which have been left untouched over the last 30 years. First, Lyons, Kaplan, Dwight, and Menyuk (LKDM) theoretically derived that the Menyuk *et al.* ferrimagnetic spiral long-range order is not a ground state.[1,3] Treating spins as classical vectors, the LKDM theory tried to solve the Heisenberg Hamiltonian for a cubic normal spinel system. A solution of a ferrimagnetic spiral long-range configuration was assumed, and the cone angles were calculated as a function of u, where the parameter u is defined as

$$u = \frac{4J_{BB}S_BS_B}{3J_{AB}S_AS_B}. \quad (1)$$

Here, J_{AB} is an antiferromagnetic exchange integral between the nearest-neighbor spins at the *A* and *B* sites, J_{BB} is that between the nearest-neighbor spins at the two *B* sites, and S_A and S_B are magnitudes of the spins at the *A* and *B* sites, respectively. The cone angles experimentally obtained by Menyuk *et al.* correspond to a u value of 2.0.[1] However, the ferrimagnetic spiral long-range configuration in the region where $u > 1.298$ was shown to be locally unstable with respect to arbitrary small deviations of all the spin vectors from their original directions. LKDM and Menyuk *et al.* themselves gave no other model reflecting the local instability, and only commented that the ferrimagnetic spiral long-range order should be taken as a first approximation.[1]

Second, Plumier suggested a possibility of ferrimagnetic spiral short-range order below T_S by analyzing his neutron powder diffraction data, though he did not mention whether this short-range order was due to both magnetic components or to only one of them.[4] The reason for this suggestion is that the magnitude of magnetic moments could not be explained within a long-range order model.[4] The experimental values were obtained as $1.253\mu_B$ for the Co^{2+} ion and $1.369\mu_B$ for the Cr^{3+} ion.[4] These values were too small compared to the spin-only values of $3\mu_B$ for both magnetic ions.[4] Nevertheless, no definitive data showing whether magnetic order is a

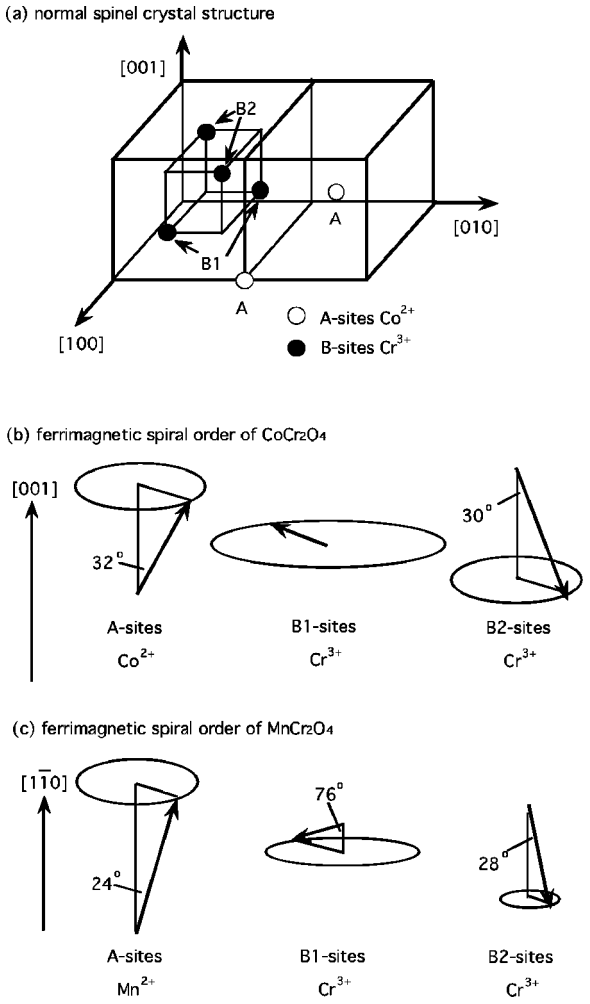

FIG. 1. (a) Sublattices *A*, *B*1, and *B*2 in a chemical unit cell. Atomic sites of oxygen ions are omitted. (b) Ferrimagnetic spiral order of $CoCr_2O_4$ below T_S obtained in the previous neutron powder diffraction experiments (Ref. 1). The ferrimagnetic component of spins is ferromagnetic in each sublattice, and points to the [001] direction. The spiral component of spins is described by propagation vector $Q=(0.62,0.62,0)$, and lies within the (001) plane. (c) Ferrimagnetic spiral order of $MnCr_2O_4$ below T_S obtained in the previous neutron powder diffraction experiments (Ref. 2). The ferrimagnetic component of spins is ferromagnetic in each sublattice, and points to the $[1\bar{1}0]$ direction. The spiral component of spins is described by propagation vector $Q=(0.59,0.59,0)$, and lies within the $(1\bar{1}0)$ plane.

long-range order or a short-range order have been obtained so far.

On the other hand, the same problems are outstanding for the similar cubic normal spinel ferrimagnet $MnCr_2O_4$, in which magnetic Mn^{2+} ions occupy *A* sites and magnetic Cr^{3+} ions occupy *B* sites.[2] Hastings *et al.* performed neutron powder diffraction experiments, and reported that magnetic order of $MnCr_2O_4$ is also composed of a ferrimagnetic component and a spiral component and the two components exhibit long-range orders below $T_C \simeq 43$ K and $T_S \simeq 18$ K, respectively.[2] The ferrimagnetic spiral long-range order below T_S is shown in Fig. 1(c). However, the cone angles lead to a *u* value of 1.6, which again belongs to the locally unstable region in the LKDM theory.[2] Furthermore, the intensities of a group of satellite reflections corresponding to the spiral component are too weak compared to those of the fundamental reflections corresponding to the ferrimagnetic component. The contradiction of the intensities, which is identical to the inconsistency of the magnitude of magnetic moments within a framework of magnetic long-range order, were also pointed out by Plumier.[4]

In fact, these subjects of the local instability in the LKDM theory and Plumier's short-range order model have been regarded as irrelevant. Actually, Plumier speculated that the ferrimagnetic spiral short-range order is derived by taking into account more exchange integrals in the LKDM theory, not by the local instability of the ferrimagnetic spiral long-range order.[4] On the contrary, we expect that the local instability generates a magnetic short-range order in $CoCr_2O_4$ and $MnCr_2O_4$.

In the present paper, we reinvestigate the ferrimagnetic spiral order of $CoCr_2O_4$ and $MnCr_2O_4$ by neutron scattering experiments and magnetization measurements on single crystal specimens. In Sec. II, the experimental methods are described. In Sec. III A 1, neutron data of $CoCr_2O_4$ reveal that fundamental reflections are coherent Bragg reflections while satellite reflections are diffusive at 8 K. Since the ferrimagnetic component is observed as fundamental reflections and the spiral component is observed as satellite reflections separately in neutron scattering experiments, the data indicate that ferrimagnetic long-range order and spiral short-range order coexist at 8 K. In Sec. III A 2, the mean values of cone angles of the ferrimagnetic spiral order of $CoCr_2O_4$ at 8 K are obtained by analyzing the experimental intensity of 21 satellite reflections. In Sec. III B, it is found that magnetization of $CoCr_2O_4$ behaves like reentrant-spin-glass (RSG) in $CoCr_2O_4$. In Secs. III C and III D, neutron and magnetization data of $MnCr_2O_4$ that are similar to those of $CoCr_2O_4$ are reported. In Sec. IV A, *u* values in the LKDM theory are estimated from the present cone angles and the spiral short-range order in the two chromites is discussed in the light of the local instability. In Sec. IV B, the RSG-like behavior of the ferrimagnetic domains is explained as coming from freezing and fluctuation of the spiral component. In Sec. IV C, we propose the concept of weak magnetic geometrical frustration (weak MGF) by combining the local instability with usual MGF, and comprehensively interpret the spiral short-range order in the two materials. The conclusions are summarized in Sec. V.

II. EXPERIMENTS

Single crystals of $CoCr_2O_4$ and $MnCr_2O_4$ were prepared by K. Kohn (Waseda University) using the flux method. Other single crystals grown in the same batches were ground into powder for x-ray diffraction experiments. No extra lines, which could not be explained by the spinel structure, were observed in the x-ray powder diffraction patterns of the two powder specimens at room temperature. Single crystals *A* and *B* ($CoCr_2O_4$), the size of which is about $6\times6\times4$ and $5\times3\times1$ mm^3, were used for neutron scattering experiments

and magnetization measurements, respectively. Some other single crystals of $CoCr_2O_4$ obtained from the same batch were previously studied by neutron scattering and magnetoelectric effect measurements.[5,6] Single crystals *C* and *D* ($MnCr_2O_4$), the size of which is $2\times2\times2$ and $1\times1\times1$ mm^3, were used for neutron scattering experiments and magnetization measurements, respectively.

Neutron scattering experiments were performed on the T1-1 triple axis spectrometer installed at a thermal guide of JRR-3M, Tokai, Japan. The energy of the incident neutrons was fixed at 13.5 meV. A pyrolytic graphite filter efficiently eliminated higher-order contamination. The horizontal collimator sequence was set to open-20′-20′-40′ for measuring the line profile of a fundamental and a satellite reflection [Figs. 13(a), 13(b), and 16(a)] and to open-40′-40′-40′ for all the other scans. Single crystals *A* and *C* were mounted on the cold finger of a He flow cryostat or of a He closed-cycle refrigerator.

Static magnetization measurements were performed in a superconducting quantum interference device system at the Materials Characterization Central Laboratory, Waseda University, Japan. A magnetic field was applied to single crystals *B* and *D* along the [001] and $[1\bar{1}0]$ directions, which are the easy axis of the ferrimagnetic component of $CoCr_2O_4$ and that of $MnCr_2O_4$, respectively.[1,2]

III. RESULTS

In the following sections, *hkl* stands for the peak position of the fundamental reflection at the *hkl* reciprocal lattice point (RLP), and *hkl*(±) symbolizes peak positions of the satellite reflections at the $hkl\pm Q$ RLPs. Here, *Q* represents the propagation vector of the spiral component, which is parallel to the [110] direction.

A. Neutron scattering experiments of $CoCr_2O_4$

1. Magnetic reflections at 8 K

Figure 2(a) shows the line profile of the 220 fundamental reflections at 150 K ($T>T_C$)) and 8 K. At both temperatures, the 220 fundamental reflections are coherent Bragg reflections, indicating that the ferrimagnetic component exhibits long-range order (>50 nm, a resolution limit in the present experiments) at 8 K. Figure 2(b) shows scan data around the 220(−) RLP at 150 and 8 K. The satellite reflection at 8 K is diffusive, meaning that the spiral component exhibits short-range order at 8 K. The diffusive line profile is well fitted by a Lorentzian, with a half width half maximum (HWHM) κ value of 0.042 ($2\pi/a$ unit) after correction of the Cooper and Nathans' resolution function.[7] The correlation length of the spiral component ξ is estimated to be 3.1 nm by taking the inverse of κ.

We also recorded the line profile of the 220(−) satellite reflection, studied at 8 K in a magnetic field of 3000 Oe after cooling in the same magnetic field. A single ferrimagnetic domain state is expected to develop in the magnetic field, because the magnitude of 3000 Oe is more than twice as large as that of the coercive force at 8 K as shown in Sec.

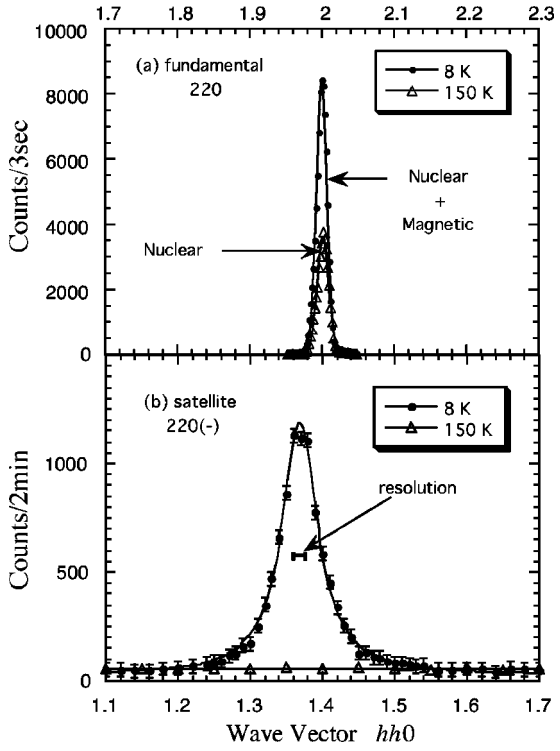

FIG. 2. Neutron scattering data of $CoCr_2O_4$ obtained by scanning along the [110] direction around the 220 reciprocal lattice point (a) and the 220(−) reciprocal lattice point (b) at 150 K ($T>T_C$) and 8 K. In (b), the solid line is drawn by fitting the experimental data at 8 K with a Lorentzian.

III B. The line profile of the 220(−) satellite reflection in the magnetic field is compared to that obtained without a magnetic field in Fig. 3. Since the satellite reflection in the magnetic field is again diffusive, the spiral short-range order is maintained even in the single ferrimagnetic domain state. The linewidth κ and the correlation length ξ at 8 K in the magnetic field are estimated to be 0.038 ($2\pi/a$ unit) and 3.5 nm, respectively.

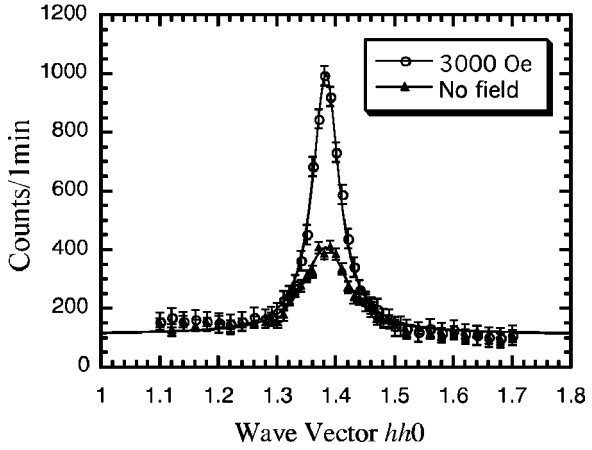

FIG. 3. Neutron scattering line profiles of the satellite reflection of $CoCr_2O_4$, studied at 8 K in a magnetic field of 3000 Oe and without a magnetic field. The scattering intensity in the magnetic field is about three times the one without a magnetic field because the magnetic field produces a single ferrimagnetic domain state.

TABLE I. Experimental intensity and best-fit calculated intensity of 21 satellite reflections of $CoCr_2O_4$ at 8 K. The calculated intensity was obtained from the ferrimagnetic spiral model of Fig. 4.

hkl	Experimental	Calculated
000(+)	<31	32
220(−)	1000	872
220(+)	533	466
440(−)	<21	14
111(−)	<25	3
111(+)	<25	2
331(−)	<23	2
331(+)	<23	1
002(+)	529	628
222(−)	75	52
222(+)	126	66
442(−)	216	178
113(−)	127	257
113(+)	104	159
333(−)	60	97
333(+)	81	74
004(+)	448	531
224(−)	116	138
224(+)	<26	25
$2\bar{2}0(+)$	110	100
$0\bar{4}0(+)$	143	149

2. Mean values of cone angles of ferrimagnetic spiral order at 8 K

In order to estimate mean values of cone angles, we measured the scattering intensity of 21 satellite reflections at 8 K without a magnetic field. Table I gives the experimental intensities. The intensity was calculated so as to fit the experimental values by varying the cone angles in a least squares method on the basis of a long-range order model for simplicity. In the calculations, the Watson-Freeman magnetic form factors of the Co^{2+} and Cr^{3+} ions were used, and the secondary extinction effect was ignored because the satellite reflections were diffusive. The magnitudes of the magnetic moments of the Co^{2+} and Cr^{3+} ions were assumed to be their spin-only values of $3\mu_B$, as in the Menyuk *et al.* analysis.[1] Although there are four propagation vectors along the $\pm[110]$ and $\pm[\bar{1}10]$ directions for the ferrimagnetic domain with spontaneous magnetization along the [001] direction,[1] the multiplicity of spiral clusters was not taken into account. The reason is that scattering from many spiral clusters is resolved in accordance with their propagation vectors in neutron scattering experiments on a single crystal. Actually, the positions of the satellite reflections in Table I are described by only two propagation vectors along the $\pm[110]$ directions, symbolized by (+) and (−). In this way, we obtained the best-fit calculated intensity given in Table I and the mean values of the cone angles shown in Fig. 4.

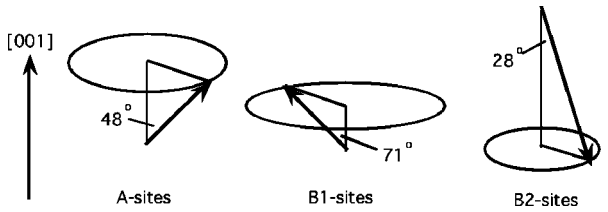

FIG. 4. Mean ferrimagnetic spiral order of $CoCr_2O_4$ estimated by the present neutron scattering experiments.

3. Temperature dependence

We measured the temperature dependence of the 111 fundamental reflection and of the 220(−) satellite reflection. Figure 5 shows the temperature dependence of the integrated intensity of the 111 fundamental reflection. As the temperature decreases below room temperature, the magnetic component of the fundamental reflection appears at $T_C \simeq 93$ K, its intensity increases until $T_S \simeq 24$ K and then slightly decreases. This slight decrease means that the magnetic moments tilt only 1° further with decreasing the temperature from T_S to 8 K.

In the whole temperature range of the present neutron scattering experiments, the fundamental reflection was a coherent Bragg reflection. Hence, the ferrimagnetic component exhibits long-range order at all temperatures below T_C.

Figure 5 also shows the temperature dependence of the peak intensity of the 220(−) satellite reflection. The weak satellite reflection can be observed from 50 K onwards and, as the temperature decreases further, the peak intensity gradually increases and almost saturates at $T_F \simeq 13$ K.

The anomaly at T_S is not identical to a ferrimagnetic to ferrimagnetic-spiral transition, because the tilt of only 1° contradicts the mean values of the cone angles illustrated in Fig. 4. Menyuk *et al.* reported that the spiral short-range order exists below $T_t \simeq 86$ K, far above T_S.[1] In addition, the present result that the satellite reflection is too weak to be observed above 50 K implies that the spiral component fluctuates dynamically retaining the correlation above T_S. Note that all the above neutron data were studied by neutron *elastic* scattering; only the spiral component fluctuating slower than the energy resolution is observable as elastic scattering.

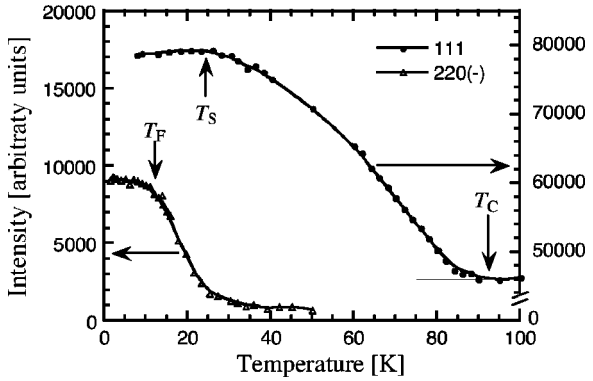

FIG. 5. Temperature dependence of the integrated intensity of the 111 fundamental reflection and temperature dependence of the peak intensity of the 220(−) satellite reflection of $CoCr_2O_4$.

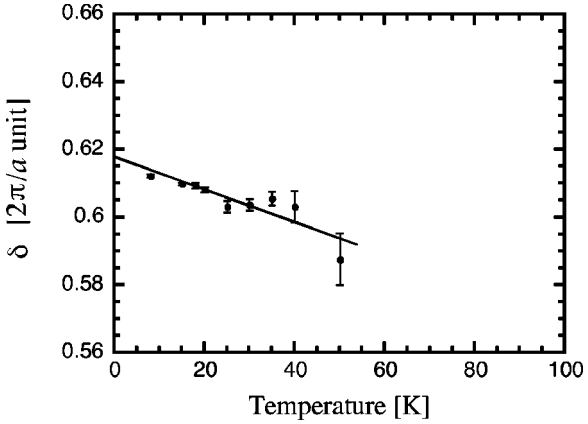

FIG. 6. Temperature dependence of δ of $CoCr_2O_4$, where propagation vector $\mathbf{Q}=(\delta,\delta,0)$.

The dynamics of the spiral component is more quantitatively investigated by inelastic neutron scattering in the later paragraphs.

Figure 6 shows the temperature dependence of δ, where $Q=(\delta,\delta,0)$. As the temperature decreases, the peak position of the 220(−) satellite reflection slightly shifts towards the origin 000 in the reciprocal lattice space. The value of δ, linearly extrapolated to 0 K, is 0.616. The period of the spiral order is incommensurate with the lattice periodicity.

Neither extra commensurate peaks with $\delta=2/3$ nor any incommensurate-commensurate transition of δ around $T_I=12.5$ K, reported by Plumier[4] and Funahashi *et al.*,[5] were observed. Therefore, the origin of the anomaly at T_F differs from that of the transition at T_I, and the value of T_F only happens to be very close to that of T_I. In contrast, the present value of 0.616 is consistent with Menyuk's value of 0.62.[1] No evidence of such a magnetic transition around T_I, which is accompanied with a change of magnetic symmetry, was also found in the magnetoelectric effect measurements on single crystals after cooling in electric and magnetic fields applied simultaneously.[6] With regard to the discrepancy on whether the spiral order is incommensurate or commensurate with the lattice periodicity, Dwight and Menyuk suggested that the commensurate spiral order is caused by some defects because only the incommensurate spiral order could be theoretically derived.[8] According to their reports,[8] the present sample includes less defects than those of Menyuk *et al.*[1] and of Kaneko *et al.*[6]

Figure 7(a) shows the temperature dependence of the linewidth κ of the 220(−) satellite reflection. As the temperature decreases, the linewidth gradually decreases and becomes almost constant at T_F. Figure 7(b) shows the temperature dependence of the correlation length of the spiral component $\xi=1/\kappa$. As the temperature decreases, the value of ξ, which is about 0.8 nm at 50 K, increases and almost saturates around 3.1 nm at T_F.

Figure 8(a) shows energy spectra at the 220(−) RLP at 35 and 8 K. The spectrum line at 35 K is broader than the resolution measured by using a vanadium standard sample, while the spectrum line at 8 K is as sharp as the resolution. The temperature dependence of the linewidth of the spectrum line after correction of the resolution is shown in Fig. 8(b). The

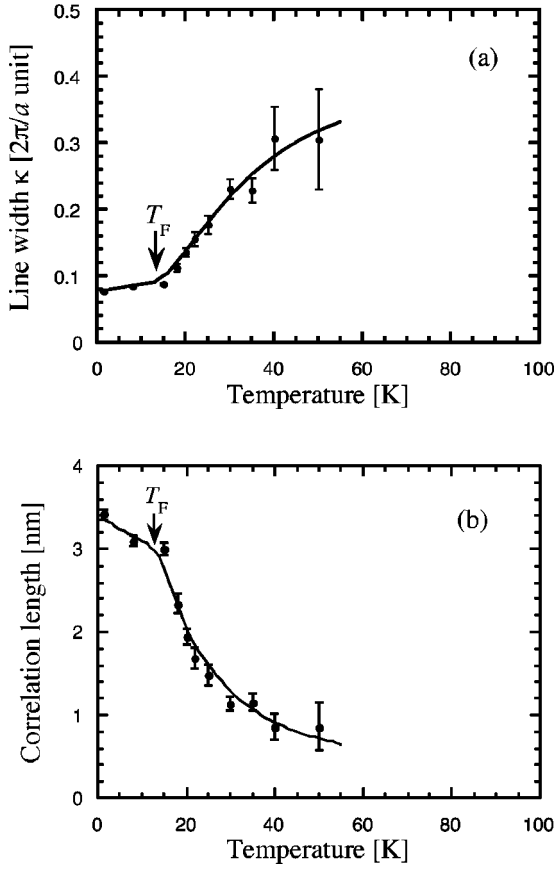

FIG. 7. (a) Temperature dependence of the linewidth of the satellite reflection of $CoCr_2O_4$ after correction of the Cooper and Nathans' resolution function (Ref. 7). (b) Temperature dependence of the correlation length of the spiral component. The values are obtained by taking the inverse of the linewidth.

linewidth is estimated by a Gaussian fit for simplicity. As the temperature decreases, the linewidth becomes small and falls within the statistical error of ~10 GHz at $T_S'\simeq 18$ K.

Although the energy spectrum line is quasielastic (not elastic) above T_S', the satellite reflection does not mean the spin wave of the ferrimagnetic component. If the scattering from the spin wave causes the satellite reflection, two peaks showing the dispersion relation of the spin wave should be detected around the 220(−) RLP by a constant-energy scan of inelastic scattering experiments. Figure 9 shows a constant-energy-scan data of the 220(−) satellite reflection at 60 K. The energy transfer is fixed at 3 and 6 meV. No spin-wave peaks are detected in both data. Therefore, the incommensurate component is identified by the spiral component and not the spin wave.

B. Magnetization measurements of $CoCr_2O_4$

Figure 10 shows the temperature dependence of magnetization studied after zero field cooling (ZFC) and field cooling (FC). A magnetic field of 100 Oe was applied. The FC curve shows an anomaly around T_S, similar to the Menyuk *et al.* data.[1] However, the ZFC curve, which has not been reported so far, does not follow the same path as the FC

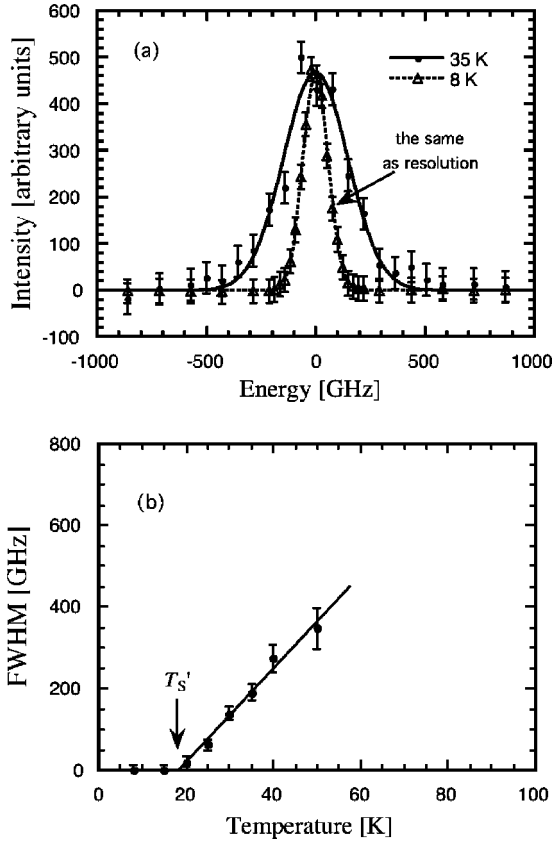

FIG. 8. (a) Energy spectra of $CoCr_2O_4$ measured at the 220(−) reciprocal lattice point at 35 and 8 K. The contribution of the incoherent scattering is subtracted from the raw data. Both data are fitted by a Gaussian for simplicity. (b) Temperature dependence of the linewidth with respect to energy (frequency) after correction of the resolution. Note that 1 meV=240 GHz.

curve like in RSG. As the temperature decreases, the ZFC curve splits from the FC one below T_t, abruptly falls below T_S', and finally saturates at T_F. The anomaly at T_S' and T_F on the ZFC curve was also confirmed in initial magnetization

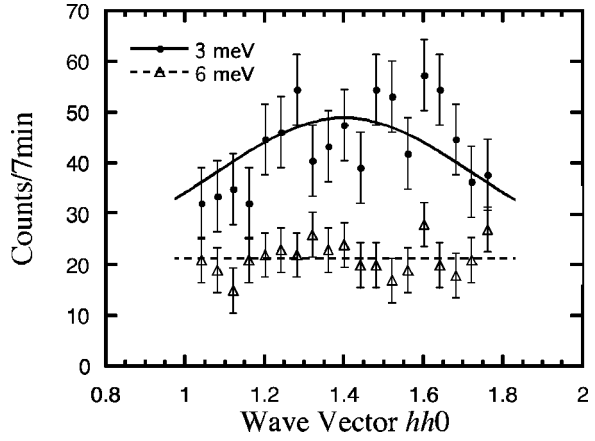

FIG. 9. Constant-energy scan of $CoCr_2O_4$ measured around the 220(−) reciprocal lattice point at 60 K. The energy transfer is fixed at 3 and 6 meV. The quasielastic scattering is still observed at 3 meV and no appreciable peak is observed at 6 meV.

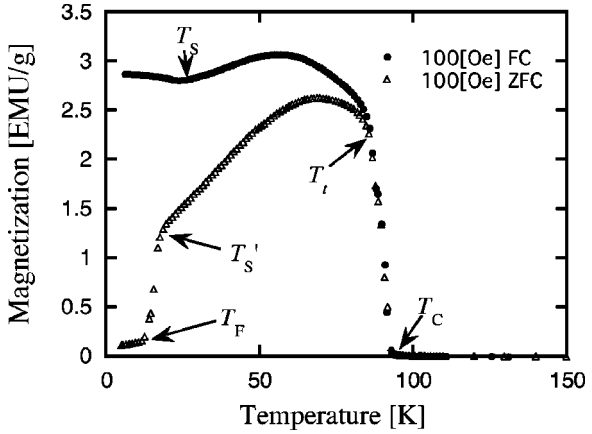

FIG. 10. Temperature dependence of magnetization of $CoCr_2O_4$ studied both after zero field cooling (ZFC) and field cooling (FC). A magnetic field of 100 Oe was applied.

data and coercive force data. Figure 11 shows initial magnetization curves at several temperatures after ZFC. The initial magnetization readily responds to the applied magnetic field for temperatures above T_S', but requires a larger field at lower temperature. In particular, at 5 K ($T<T_F$), it hardly increases below 1700 Oe. Figure 12 shows the temperature dependence of the coercive force. As the temperature decreases, the coercive force begins to increase dramatically from T_S' and the slope becomes steeper at T_F.

Thus, the response of the ferrimagnetic domains becomes harder to the applied magnetic field at T_t, T_S, and T_F with decreasing temperature.

C. Neutron scattering experiments of $MnCr_2O_4$

The line profiles of magnetic reflections of $MnCr_2O_4$ are very similar to those of $CoCr_2O_4$. Figure 13(a) shows the line profiles of the 220 fundamental reflections at 60 K ($T>T_C$) and 4 K. Both reflections are coherent Bragg reflections, meaning that the ferrimagnetic component exhibits long-range order (>50 nm) below T_C. Figure 13(b) shows the line profile of the 220(−) satellite reflection at 4 K and scan data

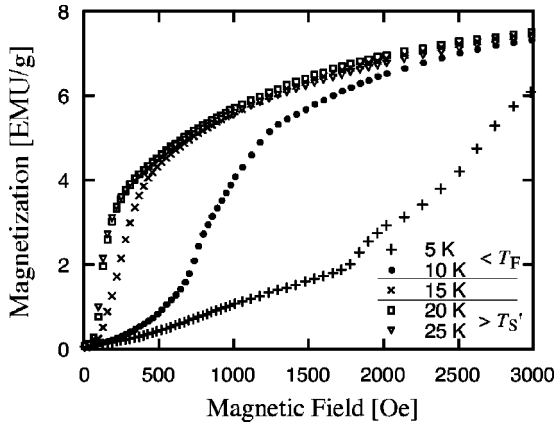

FIG. 11. Initial magnetization curves of $CoCr_2O_4$ studied at several temperatures.

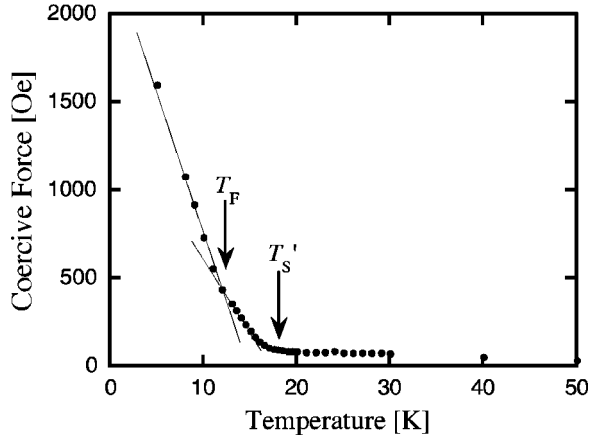

FIG. 12. Temperature dependence of the coercive force of $CoCr_2O_4$.

along the [110] direction around the 220(−) RLP at 30 K ($T > T_S$). The satellite reflection is diffusive at 4 K, indicating that the spiral component exhibits short-range order at 4 K as that of $CoCr_2O_4$. The diffusive line profile is also described by a Lorentzian. The only difference from $CoCr_2O_4$ is that the HWHM of the scattering function of the

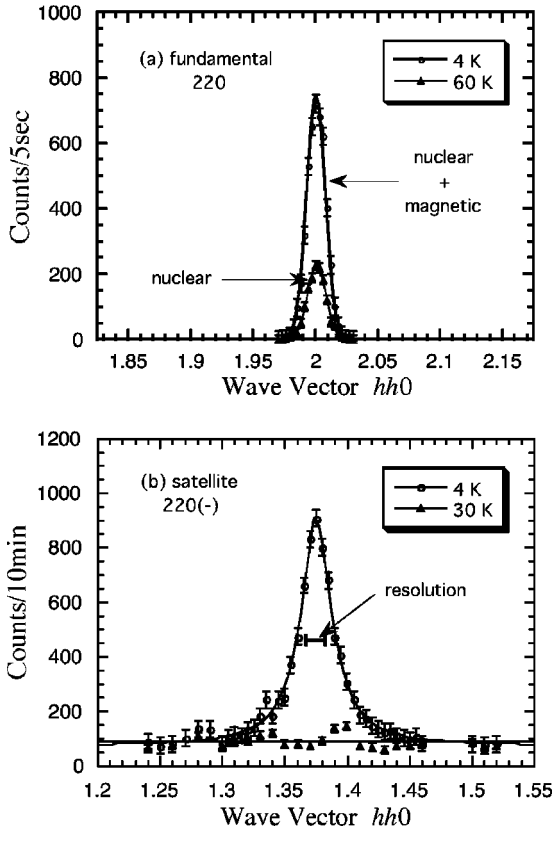

FIG. 13. Neutron scattering data of $MnCr_2O_4$ obtained by scanning along the [110] direction around the 220 reciprocal lattice point at 60 K ($T > T_C$) and 4 K (a) and around the 220(−) reciprocal lattice point at 30 K ($T > T_S$) and 4 K (b). In (b), the solid line is drawn by fitting the experimental data at 4 K with a Lorentzian.

TABLE II. Experimental intensity and best-fit calculated intensity of satellite reflections of $MnCr_2O_4$ at 4 K. The calculated intensity is obtained from the ferrimagnetic spiral model of Fig. 14.

hkl	Experimental	Calculated
000(+)	<50	0
220(−)	1000	978
220(+)	489	524
440(−)	<30	1
111(−)	<37	38
111(+)	<37	29
002(+)	301	323
222(−)	155	119
113(−)	108	104
113(+)	158	78
333(−)	<37	56

satellite reflection κ is estimated to be 0.014 ($2\pi/a$ unit), giving the correlation length of the spiral component $\xi = 9.9$ nm on average at 4 K.

The propagation vector of the spiral component Q is estimated to be $(0.626 \pm 0.009, 0.626 \pm 0.009, 0)$ and is independent of the temperature within statistical uncertainties in the present experiments. On the other hand, Dwight *et al.*, Hastings *et al.*, and Plumier reported the values of (0.64,0.64,0), (0.59,0.59,0), and $(\frac{2}{3}, \frac{2}{3}, 0)$ by neutron powder diffraction, respectively.[2,4,9] The Dwight *et al.* value of (0.64,0.64,0) is consistent with the present value within the resolution width. The Hastings *et al.* value of (0.59,0.59,0) is also compatible with the present value because the resolution of scattering angle is estimated to be about 0.5°, which gives a value of $(0.59 \pm 0.05, 0.59 \pm 0.05, 0)$, by considering the linewidth of Bragg reflections in the Hastings *et al.* neutron powder diffraction experiments.[2] Although Plumier's commensurate value of $(\frac{2}{3}, \frac{2}{3}, 0)$ disagrees with the present value, it would appear that the commensurate spiral order is caused by some defects as mentioned for $CoCr_2O_4$ in Sec. III A 3.[8]

Table II gives the experimental scattering intensities of 11 satellite reflections at 4 K. Mean values of cone angles at 4 K were estimated from these intensities on the same assumption of $CoCr_2O_4$ in Sec. III A 2 except that the magnitude of the magnetic moment of Mn^{2+} ions was fixed at its spin-only value of $5\mu_B$. The best-fit calculated intensities and the mean values of the cone angles are given in Table II and Fig. 14, respectively.

Figure 15 shows the temperature dependences of the integrated intensity of the 111 fundamental reflection and of

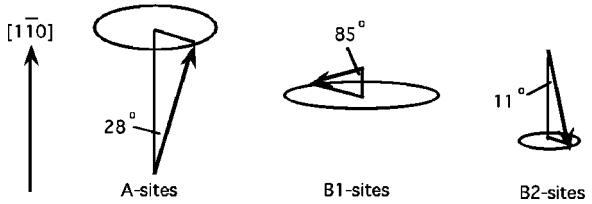

FIG. 14. Mean ferrimagnetic spiral order of $MnCr_2O_4$ estimated by the present neutron scattering experiments.

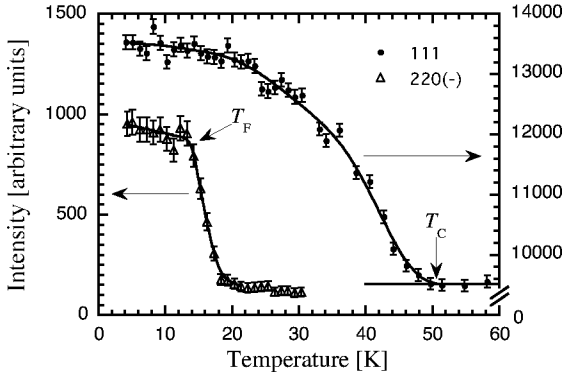

FIG. 15. Temperature dependences of the integrated intensity of the 111 fundamental reflection and of the peak intensity of the 220(−) satellite reflection.

the peak intensity of the 220(−) satellite reflection. As the temperature decreases below room temperature, the magnetic component of the fundamental reflection appears at $T_C \simeq 51$ K, and gradually increases below T_C. No slight decrease below T_S reported for $CoCr_2O_4$ (Fig. 5) is observed within statistical uncertainties. The weak satellite reflection is observed from around 20 K, and the intensity of the satellite reflection rapidly increases with decreasing temperature and saturates below $T_F \simeq 14$ K.

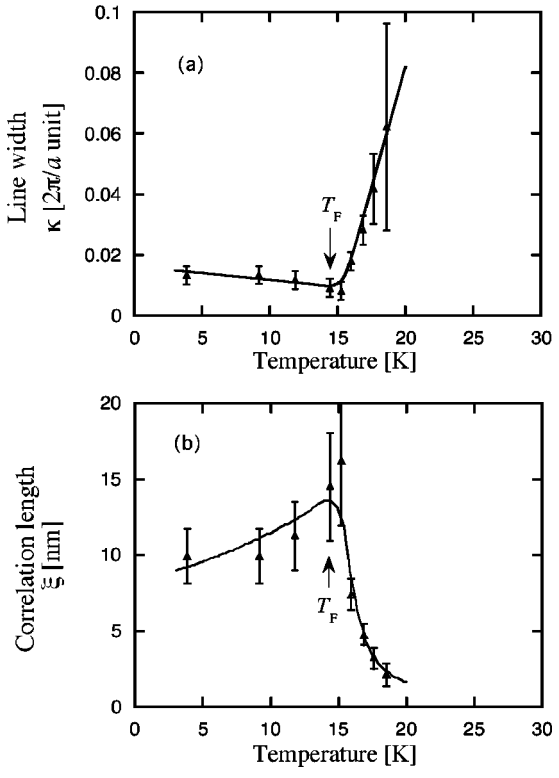

FIG. 16. (a) Temperature dependence of the linewidth of the satellite reflection of $MnCr_2O_4$ after correction of the Cooper and Nathans resolution function (Ref. 7). (b) Temperature dependence of the correlation length of the spiral component. The values are obtained by taking the inverse of the linewidth.

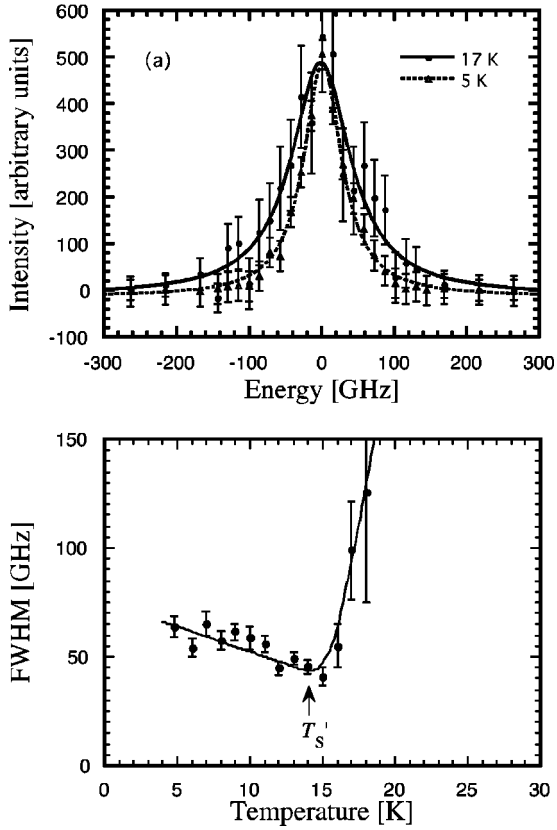

FIG. 17. (a) Energy spectra of $MnCr_2O_4$ measured at the 220(−) reciprocal lattice point at 17 and 5 K. The contribution of the incoherent scattering is subtracted from the raw data. Both data are simply fitted by a Lorentzian. (b) Temperature dependence of the linewidth of the energy spectra without the correction of resolution.

Figures 16(a) and 16(b) show the temperature dependences of the HWHM of the satellite reflection κ and of the correlation length of the spiral component $\xi = 1/\kappa$, respectively. As the temperature decreases, the value of κ decreases towards T_F and slightly increases around 0.011 ($2\pi/a$ unit) below T_F. The value of ξ is estimated to around 3 nm at 18 K, increases towards T_F, and slightly decreases around 12 nm below T_F when decreasing the temperature.

Figure 17(a) shows energy spectra at the 220(−) RLP at 17 and 5 K. The spectrum line studied at 17 K is broader than that studied at 5 K. The linewidth of the two energy spectra is sharper than that measured by using incoherent scattering from a vanadium standard sample because the satellite reflection is barely diffusive in the k space (almost coherent Bragg scattering). As noted by Cooper and Nathans, only the section of a resolution ellipsoid at $\delta Q = 0$ is observed for coherent Bragg scattering, while the projection on an energy axis of a resolution ellipsoid of all δQ is observed for incoherent scattering.[7] Figure 17(b) shows the temperature dependence of the linewidth of the energy spectra. The linewidth is simply estimated by a Lorentzian fit without correction of the resolution because the experimental measurements of the incoherent scattering from a vanadium standard sample cannot be used for the correction of the energy resolution as mentioned above. However, it is indisputable that

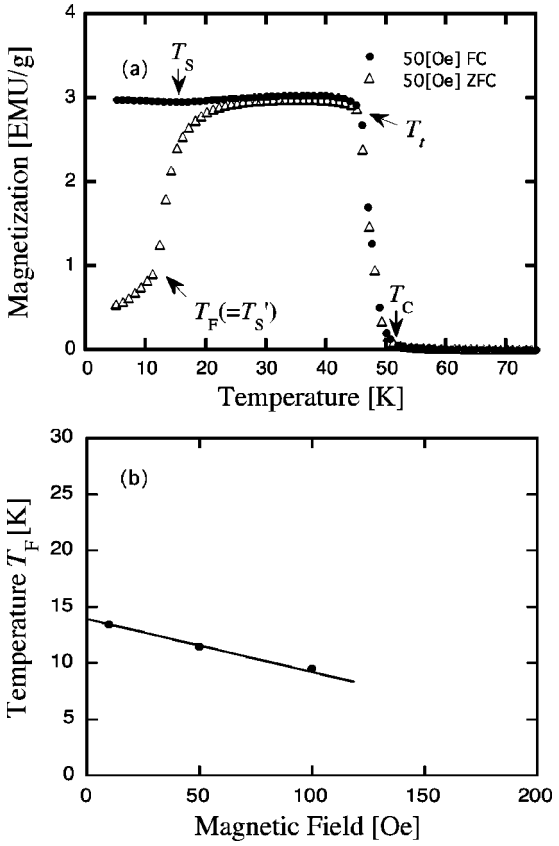

FIG. 18. (a) Temperature dependence of magnetization of $MnCr_2O_4$ studied both after zero field cooling (ZFC) and field cooling (FC). A magnetic field of 50 Oe was applied. (b) Magnetic field dependence of the value of T_F.

the linewidth decreases with decreasing temperature and exhibits anomaly at $T_S' \simeq 14$ K. The value of T_S' is equal to that of T_F in $MnCr_2O_4$ within statistical uncertainties.

D. Magnetization measurements of $MnCr_2O_4$

Magnetization of $MnCr_2O_4$ also exhibits RSG-like behavior and anomaly at T_t and $T_S' = T_F$. Figure 18(a) shows the temperature dependence of magnetization of $MnCr_2O_4$ studied after zero field cooling and field cooling. A magnetic field of 50 Oe was applied. As the temperature decreases, the FC curve abruptly uprises at T_C, is almost constant below $T_t \simeq 45$ K, and exhibits a small kink at $T_S \simeq 16$ K. However, the ZFC curve, which has not been reported so far, does not trace the same path as the FC curve. As the temperature decreases, the ZFC curve splits from the FC one below $T_t \simeq 45$ K, abruptly falls below around 20 K, and slowly descends below $T_F(50\ \text{Oe}) \simeq 12$ K. The value of $T_F(H)$ increases with decreasing magnetic field H and is extrapolated to 14 K at 0 Oe [Fig. 18(b)], which corresponds to the value of T_F obtained by neutron scattering without a magnetic field.

Figure 19 shows the temperature dependence of the coercive force of $MnCr_2O_4$. The coercive force increases below $T_S' = T_F$.

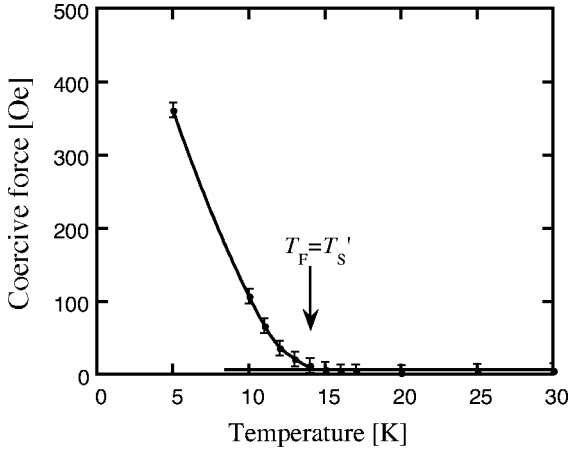

FIG. 19. Temperature dependence of the coercive force of $MnCr_2O_4$.

IV. DISCUSSION

A. Ferrimagnetic long-range order and spiral short-range order below T_F

The present neutron scattering experiments revealed that the ferrimagnetic long-range order and the spiral short-range order coexist below T_F in $CoCr_2O_4$ and $MnCr_2O_4$. The correlation length of the ferrimagnetic order is larger than a resolution limit of 50 nm, while that of the spiral order of $CoCr_2O_4$ and $MnCr_2O_4$ is estimated to around 3.1 and 9.9 nm below T_F, respectively. Therefore, we can depict the schematic picture Fig. 20, in which many spiral clusters represented by different Qs are distributed in a single ferrimagnetic domain. In $CoCr_2O_4$, there are the four spiral propagation vectors along the $\pm[110]$ and $\pm[1\bar{1}0]$ directions for an easy axis along the [001] direction.[1] Such coexistence is compatible with the fact that signals in magnetoelectric effect measurements of $CoCr_2O_4$ change their sign when the direction of the magnetic or electric field is reversed during magnetoelectric cooling.[6] In $MnCr_2O_4$, there are two spiral

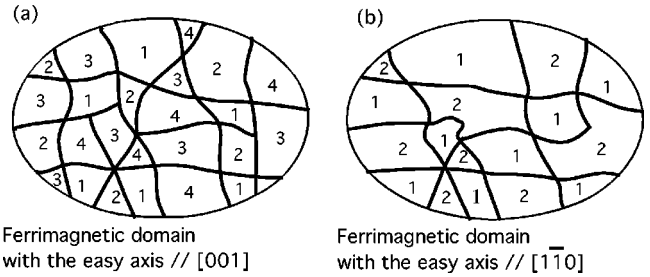

FIG. 20. Schematic of the coexistence of the spiral clusters with different Qs in a ferrimagnetic domain (>50 nm) of: $CoCr_2O_4$ (a) and of $MnCr_2O_4$ (b). In (a) the mean size of the spiral clusters is estimated to be 3.1 nm. The symbols 1, 2, 3, and 4 stand for the four Qs along the [110], $-[110]$, $[1\bar{1}0]$, and $-[1\bar{1}0]$ directions, respectively. In (b), the mean size of the spiral clusters is estimated to be 9.9 nm. The symbols 1 and 2 mean the two Qs along the [110] and $-[110]$ directions, respectively.

propagation vectors along the $\pm[110]$ directions for an easy axis along the $[1\bar{1}0]$ direction.[2]

We also estimated the mean values of the cone angles of the ferrimagnetic spiral order of $CoCr_2O_4$ and $MnCr_2O_4$, illustrated in Figs. 4 and 14. The present cone angles are different from the previous ones shown in Figs. 1(b) and 1(c). The reason is most likely that the constraint of the LKDM theory was released in the present calculations. The previous cone angles were obtained by selecting a set which best fits their neutron powder diffraction pattern, only from the sets derived from the LKDM theory.[1,2] Since the LKDM theory assumed only the ferrimagnetic spiral long-range configuration as a solution and only two nearest-neighbor exchange integrals J_{AB} and J_{BB},[3] the present cone angles would be derived by taking into account solutions of magnetic short-range order and more exchange integrals between the *A* site and the *B* site, the *B* site and the *B* site, and the *A* site and the *A* site in addition to J_{AB} and J_{BB}.

The u value cannot be strictly defined from the present cone angles owing to the absence of the constraints of the LKDM theory. In spite of this, we transform the three cone angles into three u values by using the results of the LKDM theory and take the average $\langle u\rangle$ of the three u values for each material, in order to discuss the local instability of the ferrimagnetic spiral long-range order in some way. The cone angles at *A* sites, *B*1 sites, and *B*2 sites of $CoCr_2O_4$ correspond to $u=2.9$, 1.4, and 1.7, respectively. Hence, the value of $\langle u\rangle=2.0$, which belongs to the locally unstable region in the LKDM theory and is equal to the previous value,[1] is obtained. The cone angles at *A*, *B*1, and *B*2 sites of $MnCr_2O_4$ give $u=1.8$, 1.8, and 0.96, respectively. These values lead to the value of $\langle u\rangle=1.5$, which again belongs to the locally unstable region and is close to the previous value of 1.6.[2] Therefore, we conclude that the local instability prevents the spiral component from exhibiting long-range order and generates the spiral short-range order in $CoCr_2O_4$ and $MnCr_2O_4$.

B. Temperature dependence

By measuring the ZFC curve of magnetization, it was found that the ferrimagnetic domains in $CoCr_2O_4$ and $MnCr_2O_4$ stepwise freeze at T_t, T_S', and T_F when decreasing temperature. However, the fundamental reflection corresponding to the ferrimagnetic component exhibits no anomaly at these temperatures. The anomaly is rather observed in the measurements of the satellite reflection corresponding to the spiral component. In the neutron data of $CoCr_2O_4$, the satellite reflection can be observed at 50 K, which is consistent with the Menyuk *et al.* report that the spiral short-range order appears at $T_t\simeq 86$ K.[1] The fluctuation reflecting on the linewidth of the energy spectra falls within $\sim$10 GHz below $T_S'\simeq 18$ K [Fig. 8(b)]. The increase of the correlation length is suppressed around 3.1 nm below $T_F\simeq 13$ K [Fig. 7(b)]. In the neutron data of $MnCr_2O_4$, no satellite reflection is detected within statistical uncertainties above 20 K, which is compatible with the fact that the splitting of the ZFC curve from the FC curve is still small between the splitting point $T_t\simeq 45$ K and around 20 K [Fig. 18(a)]. The slowing down of the fluctuation and a suppression of the increase of the correlation length are also observed at $T_S'=T_F\simeq 14$ K [Figs. 17(b) and 16(b)]. From the analogy between the ZFC curve of magnetization and the satellite reflection in the neutron data, the RSG-like behavior of the ferrimagnetic domains is due to the spiral component and not to the ferrimagnetic component itself. The growth of the spiral component makes the freezing of the ferrimagnetic domains harder; freezing and fluctuation of the spiral component cause the RSG-like behavior of the ferrimagnetic domains.

The following facts are unresolved at this stage and should be clarified in the future. (1) The correlation length of $CoCr_2O_4$ still increases while that of $MnCr_2O_4$ slightly decreases below T_F. (2) Although the anomaly at T_S' and T_F is clearly separated in $CoCr_2O_4$, the anomaly is indistinctive in $MnCr_2O_4$. The precise correction of the resolution to energy spectra probably leads to the different but near value of T_S'. A detailed scan of the satellite reflection over the (k,e) space is needed. (3) The anomaly at $T_S\simeq 24$ K on the FC curve of magnetization of $CoCr_2O_4$ shown in Fig. 10 was already reported by Menyuk *et al.*,[1] and was identified by Dwight and Menyuk as the spiral phase ordering in the sense that the differences among the spiral phases of the *A*, *B*1, and *B*2 sublattices are fixed.[8] In addition, we found, using neutron scattering, that the integrated intensity of the 111 fundamental reflection slightly decreases below T_S, which we interpret as the slight tilt of 1° with respect to the cone angles. The relation between these two facts, the spiral phase ordering and the slight tilt of the cone angles, is unknown.

C. Magnetic geometrical frustration

In Sec. IV A, the spiral short-range order in $CoCr_2O_4$ and $MnCr_2O_4$ was explained to arise from the local instability of the ferrimagnetic spiral long-range configuration in the LKDM theory. On the other hand, the *B* sites in both the materials form the pyrochlore lattice, which causes antiferromagnetic short-range order signaling magnetic geometrical frustration (MGF) in many systems, such as $ZnCr_2O_4$, $ZnFe_2O_4$, $Ho_2Ti_2O_7$, Y(Sc)Mn_2, and so on.[10–14] Therefore, we tentatively interpret the spiral short-range order in the two chromites as a kind of MGF in this section.

One problem is the fact that magnetic ions occupy the *A* sites (Co^{2+} and Mn^{2+}) besides the *B* sites (Cr^{3+}) in $CoCr_2O_4$ and $MnCr_2O_4$. It has been believed that MGF among the *B* sites is completely suppressed by the presence of magnetic ions on the other sublattices (*A* sites). Actually, magnetic ions are located only on the *B* sites in the above MGF systems.[10–14] Anderson also proposed the concept of MGF for only normal spinel systems where magnetic ions occupy the *B* sites.[15] On the contrary, we surmise that the effect of MGF still survives in $CoCr_2O_4$ and $MnCr_2O_4$, if the exchange interaction between the *A* sites and the *B* sites is smaller than that among the *B* sites. We call the phenomenon "weak magnetic geometrical frustration" (weak MGF) and distinguish it from the usual MGF.

Since the degree of MGF in $CoCr_2O_4$ and $MnCr_2O_4$ is weaker than that in the usual MGF systems, the ferrimagnetic component exhibits long-range order in the two sys-

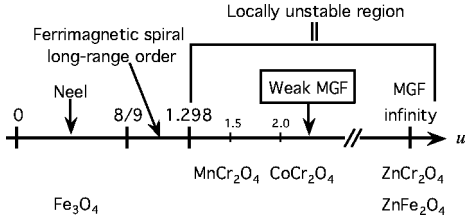

FIG. 21. The relation between the parameter u and the type of magnetism. Materials are those in cubic phases. MGF means "magnetic geometrical frustration."

tems. However, the growth of the spiral component to long-range order is prevented owing to the weak MGF, and the spiral component exhibits short-range order. The coexistence of the long-range order and the short-range order characterizes the weak MGF of $CoCr_2O_4$ and $MnCr_2O_4$.

The degree of MGF in $MnCr_2O_4$ should be weak than that in $CoCr_2O_4$ because the magnitude of magnetic moments of Mn^{2+} ions at A sites ($5\mu_B$ spin-only value) is larger than that of Co^{2+} ions at A sites ($3\mu_B$ spin-only value). The larger magnetic moments at A sites generate a stronger exchange interaction between A sites and B sites and must weaken the degree of MGF among B sites. Therefore, the correlation length of the spiral component in $MnCr_2O_4$ ($\simeq$9.9 nm) is larger than that in $CoCr_2O_4$ ($\simeq$3.1 nm).

The parameter u in the LKDM theory is useful for quantifying the degree of MGF. Figure 21 shows the magnetism of cubic normal spinel systems roughly described by the parameter u. The usual MGF corresponds to the case $u=\infty$ because $J_{AB}=0$ and $S_A=0$. As the value of u decreases below ∞, weak MGF occurs until $u=1.298$. The present systems of $CoCr_2O_4$ ($\langle u\rangle=2.0$) and $MnCr_2O_4$ ($\langle u\rangle=1.5$) belong to the weak MGF region. The fact that the $\langle u\rangle$ value of $MnCr_2O_4$ is small compared to that of $CoCr_2O_4$ is consistent with the opinion that the degree of MGF in $MnCr_2O_4$ is weaker than that in $CoCr_2O_4$. Between 1.298 and 8/9, the ferrimagnetic spiral long-range configuration sets in.[3] Below 8/9, the magnetism is described by the Néel long-range configuration.[3]

Magnetization of $CoCr_2O_4$ and $MnCr_2O_4$ behaves like RSG, while the usual MGF system shows no SG-like behavior such as $ZnFe_2O_4$.[14] Although both the MGF system and the weak MGF system would possess many degenerated or nearly degenerated ground states, the energy structure of solutions in the weak MGF system would be more complex than in the MGF system, i.e., there are probably complex barriers of potential energy between the ground states, which lead to the freezing of the spiral component and the RSG-like behavior of the ferrimagnetic domains.

V. CONCLUSIONS

We performed neutron scattering experiments on single crystals of $CoCr_2O_4$ and $MnCr_2O_4$. For both the chromites, a fundamental reflection shows a coherent Bragg peak below T_C, meaning that the ferrimagnetic component exhibits long-range order below T_C. The satellite reflection is diffusive even in the lowest temperature phase below T_F, indicating that the spiral component exhibits short-range order even below T_F. The correlation length of the ferrimagnetic order is larger than a resolution limit of 50 nm, while that of the spiral order below T_F in $CoCr_2O_4$ and $MnCr_2O_4$ is 3.1 nm (8 K) and 9.9 nm (4 K) on average, respectively.

The mean values of the cone angles below T_F illustrated in Figs. 4 and 14 were estimated by analyzing the experimental intensity of satellite reflections. The present cone angles give the average values of $\langle u\rangle=2.0$ for $CoCr_2O_4$ and of $\langle u\rangle=1.5$ for $MnCr_2O_4$. Both the values belong to the locally unstable region of the ferrimagnetic spiral long-range configuration in the LKDM theory.

Magnetization measurements on single crystals of $CoCr_2O_4$ and $MnCr_2O_4$ were also performed. The ferrimagnetic domains behave as in RSG.

The above results on spiral short-range order, local instability, and RSG-like behavior are related as follows. Since the ferrimagnetic spiral long-range configuration is locally unstable, the spiral component exhibits short-range order. The freezing and the fluctuation of the spiral component bring about the RSG-like behavior of the ferrimagnetic domains.

In addition, we proposed the concept of weak magnetic geometrical frustration (weak MGF) and classified the origin of the local instability into usual MGF and weak MGF. The weak MGF causes the spiral short-range order below T_F. Since the magnitude of magnetic moments of Mn^{2+} ions at A sites ($5\mu_B$ spin-only value) is larger than that of Co^{2+} ions at A sites ($3\mu_B$ spin-only value), the degree of MGF among the B sites in $MnCr_2O_4$ is weakened compared to that in $CoCr_2O_4$; therefore, the correlation length of the spiral component in $MnCr_2O_4$ (9.9 nm) is larger than that in $CoCr_2O_4$ (3.1 nm). The $\langle u\rangle$ value in the LKDM theory is useful for quantifying the degree of MGF and is estimated to 2.0 for $CoCr_2O_4$ and to 1.5 for $MnCr_2O_4$.

A subject of future research is to search for other weak MGF systems and to compare the data with the present data on $CoCr_2O_4$ and $MnCr_2O_4$. In particular, the weak MGF system with a larger $\langle u\rangle$ value is interesting because the $\langle u\rangle$ values of 2.0 and 1.5 for the present chromites are quite close to the critical value of 1.298. We would also like to emphasize that the concept of weak MGF can be applied not only to the chromite spinel systems but also to many other systems, including a pyrochlore lattice or a triangular lattice. Further experimental and theoretical investigations are required to develop the concept of the weak MGF.

ACKNOWLEDGMENTS

We thank Professor K. Kohn very much for supplying the single crystal specimens and giving us his helpful advice. We also thank Professor Y. Tsunoda, Professor K. Siratori, Dr. K. Kamazawa, and Professor T. A. Kaplan for fruitful discussions. This work was partially supported by a Waseda University Grant for Special Research Projects (Grant No. 2003A-589).

*Electronic address: k-tommy@aoni.waseda.jp

[1] N. Menyuk, K. Dwight, and A. Wold, J. Phys. (Paris) **25**, 528 (1964).
[2] J. M. Hastings and L. M. Corliss, Phys. Rev. **126**, 556 (1962).
[3] D. H. Lyons, T. A. Kaplan, K. Dwight, and N. Menyuk, Phys. Rev. **126**, 540 (1962).
[4] R. Plumier, J. Appl. Phys. **39**, 635 (1967).
[5] S. Funahashi, Y. Morii, and H. R. Child, J. Appl. Phys. **61**, 4114 (1987).
[6] Y. Kaneko, K. Kohn, and K. Siratori (unpublished).
[7] M. J. Cooper and R. Nathans, Acta Crystallogr. **23**, 357 (1967).
[8] K. Dwight and N. Menyuk, J. Appl. Phys. **40**, 1156 (1969).
[9] K. Dwight, N. Menyuk, J. Feinleib, and A. Wold, J. Appl. Phys. **37**, 962 (1966).
[10] S. T. Bramwell, M. J. Harris, B. C. den Hertog, M. J. P. Gingras, J. S. Gardner, D. F. McMorrow, A. R. Wildes, A. L. Cornelius, J. D. M. Champion, R. G. Melko, and T. Fennell, Phys. Rev. Lett. **87**, 047205 (2001).
[11] M. Kanada, Y. Yasui, Y. Kondo, S. Iikubo, M. Ito, H. Harashima, M. Sato, H. Okumura, K. Kakurai, and H. Kadowaki, J. Phys. Soc. Jpn. **71**, 313 (2002).
[12] H. Kadowaki, Y. Ishii, K. Matsuhira, and Y. Hinatsu, Phys. Rev. B **65**, 144421 (2002).
[13] S.-H. Lee, C. Broholm, W. Ratcliff, G. Gaasparovic, G. Huang, T. H. Kim, and S. W. Cheong, Nature (London) **418**, 856 (2002).
[14] K. Kamazawa, Y. Tsunoda, H. Kadowaki, and K. Kohn, Phys. Rev. B **68**, 024412 (2003).
[15] P. W. Anderson, Phys. Rev. **102**, 1008 (1956).